PHYSICS AND CHEMISTRY OF SOLID STATE
V.21, No.2 (2020) pp. 243-253

Vasyl Stefanyk Precarpathian National University

ФІЗИКА І ХІМІЯ ТВЕРДОГО ТІЛА
Т. 21, № 2 (2020) С. 243-253

DOI: 10.15330/pcss.21.2.243-253

UDC 544.31:546.666'24

ISSN 1729-4428

R.S. Yavorskyi

Features of Optical Properties of High Stable CdTe Photovoltaic Absorber Layer

Vasyl Stefanyk Precarpation National University, Ivano-Frankivsk, Ukraine, roctyslaw@gmail.com

In this paper, the technology of obtaining and effect of annealing on the morphology and optical properties of cadmium telluride thin films has been investigated. The effect of vacuum chamber modes on the growth of thin films has been studied. For obtained cadmium telluride thin films were used a modified thermal evaporation method deposited by Physical Vapor Deposition technique on a glass substrate with different thicknesses. The transmission measurements were carried with UV-ViS-NIR Spectrophotometer in the wavelength range 180-3300 nm, to analyze the optical properties as a function of wavelength. The optical band gap values were 1.49 eV for as-grown films and 1.46 eV after annealing. The refractive indexes of the samples were defined in the range of 2.6 – 2.8 for as-grown films and the indexes have increased after annealing depending on the wavelength region and film thickness. After annealing, the coalescence mode of growth is observed.

Keywords: thermal evaporation method, Swanepoel method, cadmium telluride thin films, optical properties, solar cells, annealing effect.

Received 14 May, 2020; Accepted 15 June 2020.

Introduction

The global Photovoltaic market has grown rapidly in the last Years [1-3]. From 2006 to 2016, the existing capacities of installed photovoltaic converters increased from 6.1 GW to 291 GW [IRENA (2018)]. During this time, the average capacity of the crystalline silicon-based photovoltaic module increased from about 12% to 17%-17.5%. This effect is because Si is stable, it relies on established process technologies with an enormous database, he delivers efficiencies in the range of (15 - 25) %, and, in general, it has proven to be reliable [4].

As we know, a thin photoactive film is deposited on a substrate, which may be either glass or a transparent film indium tin oxide (ITO) or transparent conductive oxide (TCO) [5, 6]. Compared to crystalline, thin film modules are manufactured in a single technological cycle [7]. Thin film systems production generally costs cheaper than crystalline silicon systems, but with such a scale of efficiency development in a few years, it will become competitive with crystalline silicon cells [3]. However, since thin films solar cells may offer greater opportunities for technological improvement [8].

Cadmium telluride (CdTe) is a very promising material for thin film photovoltaic (PV) devices and has a highly stable photovoltaic absorber layer [9–12]. CdTe is an AII-BVI semiconductor compound with a direct optical band gap of ~ (1.45 – 1.5) eV that is nearly optimally approaching to the solar spectrum for PV energy conversion [13, 14]. The main advantage of CdTe thin film technology is its higher production efficiency and lower production cost, compared to solar cells based on silicon wafers. This is due not only to the micron thickness of the absorbent layer but also to the low cost of the substrate on which the material is applied (preferably glass or polymer film, metal foil). [4, 8, 15].

The formation of grains, the microstructure of growing films, and, consequently, their physical properties depend on the type of deposition method used and the parameters of the process [12-13]. Heterostructure with a thickness of a few tenths of a nanometer to several micrometers can be obtained using a large number of so-called thin-film and thick-film methods. Thick-film methods are associated with the films deposition of any substance in the type of pastes or solutions prepared on its basis. Both types of technological methods provide thin-

film materials with different surface structures and a wide range of properties [16 - 19].

Not only their energy characteristics but also economic indicators are important for the thin-film technology of solar cells of a large area in terrestrial conditions. This necessitates the application of both thin film and thick film technologies methods, that satisfy such requirements as the simplicity, low cost, the ability to create homogeneous films of a large area and control of deposition process, and also allow to obtain films with certain structural, physicochemical and electro-optical properties [17].

Depending on the way of obtaining of the vapor particles, namely, using physical (thermal evaporation or ion sputtering), chemical or electrochemical processes, the following classification of thin-film cadmium telluride deposition can be made: physical vapor deposition (PVD) such as close-spaced sublimation (CSS) [20], thermal evaporation [21-25], RF magnetron sputtering [26-28], vapor transport deposition (VTD) [29, 30], metal-organic chemical vapor deposition (MOCVD) [31, 32], electro-deposition and screen printing [33, 34], pulsed laser deposition (PLD) [35, 36].

This paper presents the low-cost modified method of thermal evaporation in vacuum to produce a series of thin-film cadmium telluride as a photovoltaic absorber layer. Heterojunction thin films based on CdTe solar cells with multilayer structure (ITO/CdS/CdTe/CuO) require precise annealing process to minimize the inter-diffusion layers under during the annealing process.

I. Experimental

For Thin films of Cadmium Telluride were deposited on a cleaned glass substrate used PVD technique. The substrate temperature Ts was 470 K, the evaporation temperature of the pre-synthesized compounds CdTe changed in range (790 - 850) K. The thicknesses of the thin films defined by time of deposition τ = (160-570) sec and the deposition at 10^{-4} Pa vacuum.

The thicknesses of as-grown samples were analyzed in different places of the film by profilometer Bruker Dektak XT. Optical transmission spectra of as-grown and annealing CdTe thin films were investigated using Agilent Technologies Cary Series UV-Vis-NIR Spectrophotometer by measuring transmittance at normal incidence and room temperature. The wavelength ranges were (190 – 3300) nm with 1 nm step. Swanepoel method was used for determining optical spectra. After the measurement, the films were annealed for 90 min at 723 K in the air used Nabertherm LH04 furnace.

The surface morphology and profilograms were studied as results of AFM images analyses by the CSM Instrument technique. The size of nanoparticles in the lateral direction is determined by their height and roughness in software package Gwyddion and WSxM 5.0 Develop 8.5.

The composition properties of CdTe thin films were carried out by XRD (AXS D8 Advance, Bruker) of CuKα radiation of wavelength λ=1.540598Å in the 2θ-range 20 – 64° at a scan speed of 0.01°/min. Mathematical apparat Phase Identification from Powder Diffraction MATCH! v.3.6 was used for analysis and patterns were identified from the reference database (COD-Inorg REV204654 2018.01.02).

From transmission spectra (T) and thickness (d) taking into account the experimental error of the thin film thickness equal to ±2% and for transmittance ±1%. The error in the calculated data of the refractive index estimated at approximately ±3% and extinction coefficient ± 2.5 %.

Parameters of obtaining CdTe thin films are presented in Table I

II. Results and discussion

2.1. Technological process

The velocity of re-evaporated of atoms from a clean surface per unit area in vacuum is determined by the equation according to the Langmuir – Dashman kinetic theory [17]:

$$N_e = 2.635 \cdot 10^{20} Pe/(MT)^{1/2} \quad (1)$$

where, N_e is the evaporation rate of atoms in $cm^{-2} \cdot s^{-1}$; P_e is the equilibrium vapor pressure of evaporant under saturated vapor conditions at temperature T in K, expressed in Pa; M is the molecular weight of evaporant material. The vapor atoms condense forming a thin film after contact with the substrate.

The main parameter for the creation of technological modes for condensate depositing is the geometry of the vacuum chamber [17]. In particular, an important parameter is the temperature of evaporatoration, time of deposition, and distance between the substrate and the evaporator that sets various technological conditions for the film formation on the substrate surface [21]. The decrease of this distance is less than the mean free path of the vapor atom, and consequently, the lower vacuum is required for the deposition of a qualitative film and the growth rate, that is determined by substrate and

Table 1

The technological parameters for obtaining CdTe thin films deposited on a glass substrate

Sample No	Temperature of substrate T_S, K	Evaporation temperature T_E, K	Deposition time τ, sec	Thickness d, nm
14	470	790	300	1215
20	470	850	570	4455
21	470	820	180	1565
24	470	850	160	1215

Table 2

Characteristics of residual gas at a temperature of 297 K in a vacuum, usually created during the deposition processes of films [17, 37]

Pressure, Pa	The average mean free path of gas molecules between collisions, cm	Frequency of collisions between molecules, s^{-1}	The number of molecules colliding with the surface per unit of time, $cm^2 \cdot s^{-1}$	The number of monomolecular layers deposited during 1 s
1.33	0.5	$9 \cdot 10^4$	$3.8 \cdot 10^{18}$	4400
$1.33 \cdot 10^{-2}$	51	900	$3.8 \cdot 10^{16}$	44
$1.38 \cdot 10^{-3}$	510	90	$3.8\text{-}10^{15}$	4.4
$1.33 \cdot 10^{-5}$	$5.1 \cdot 10^4$	0.9	$3.8\text{-}10^{13}$	$4.4 \cdot 10^{-2}$
$1.33 \cdot 10^{-7}$	$5.1 \cdot 10^6$	$9 \cdot 10^{-3}$	$3.8 \cdot 10^{11}$	$4.4 \cdot 10^{-4}$

evaporator temperature, also effects on the quality of the material.

The vapor nanoparticles are scattered as a result of collisions on residual gas molecules in a vacuum system. The scattering probability is proportional to exp (-d/λ), where d is the distance between the source of evaporating matter and the substrate, and λ is the average mean free path of residual gas molecules. Also, gas molecules collide with the surface of the substrate with a velocity determined by equation (1), where parameters Pe and M relate to gas molecules with temperature T. Table 2 shows the relationship between the chamber pressure (the value of gas pressure), the mean free path value and the collisions frequency among the condensate atoms, as well as characteristics, that indicate the quality of the film. To avoid significant contamination of the films, their velocity of deposition with an average growth rate of 0.1 to 1 nm/s should be carried out at a pressure less than 10^{-3} Pa. However, at elevated temperatures, the adhesion coefficient of residual gas atoms sharply decreases, due to which it is possible already under pressure of ~ 10^{-4} Pa to obtain pure films, except for the case of deposition on easily oxidizing substances, when a higher vacuum is required.

The processes of surface diffusion control the film homogeneity in the horizontal (lateral) direction. Transport from the vapor phase (layer growth) controls the homogeneity of the film in the normal direction. The growth of a homogeneous structure can be maintained only when a sufficient number of atomic transitions between the film layers are provided during the growth process. It means that the precipitate atom on the top of the islet of growth, with high probability, can pass to the lower layer, where the potential energy is lower.

In the case of an islet growth mode (the Folmer-Weber mechanism of growth), the nucleation of small clusters occurs directly on the substrate surface, which is realized through the individual islet's formation of condensed atoms [38]. This mechanism occurs when atoms or molecules of condensate are characterized by stronger forces of interactions between each other than with material of the substrate. The opposite characteristics correspond to the Frank-van der Merwe mechanism of growth. While forming stronger bonds between condensate and substrate atoms, in comparison with the energy of interatomic bonds of the deposited substance, primary atoms during condensation form a solid monolayer on a surface that is coated with slight bound the second layer. The decrease in interlayer bonds is monotonic which tends to the bond energy value that corresponds to the bulk material. The mixed mechanism of growth or Stransky-Krastanov mechanism of growth is a sufficiently interesting intermediate case [39]. After the first monolayer or several monolayers formation, the subsequent growth of the layers becomes unfavorable: on the surface of a certain intermediate layer certain, the individual is formed. This mechanism can be caused by various technological factors, such as the choice of substrate material (molecular orientation of the substrate material), which lattice parameter or crystalline symmetry contributes to the formation of deformation tensions that prevent the next layer growth after the intermediate layer.

Modified vacuum heater was used to obtain the CdTe thin film condensates of different thickness by preset deposition temperature; the heater has a special rotation design for substrate planes occurs [21, 40]. From 1 to 15 samples with different technological parameters (substrate temperature, evaporation temperature, time of obtained), and a different substrate can be obtained in this construction. Such a system allows observing the mechanisms of the growth of thin films depending on the substrate material.

The obtaining of vapor phase semiconductor condensates in the modernized vacuum chamber (Fig. 1). The evaporator 7 is filled with a pre-synthesized CdTe compound. In advance prepared substrates 4 (for example, glass, ITO, silicon, talk) are placed on surface microheater 1. The substrate was pre-purified by chemical etching. After the shutter is blocked, the five microheaters 1 with substrates 4 and evaporator with synthesized composite are heated to preset temperature [21].

One of the microheaters places under the hole 6 in the shutter over the evaporator and provides vapor deposition on the substrate within a fixed time. Then the flow of vapor from the evaporator is blocked by the shutter and the next microheater with a substrate is rotated. In this step, the shutter opens, and the deposition is carried out with another time. The process repeats five times for each microheater of the substrate, accordingly.
In addition, the proposed device allows also the obtaining

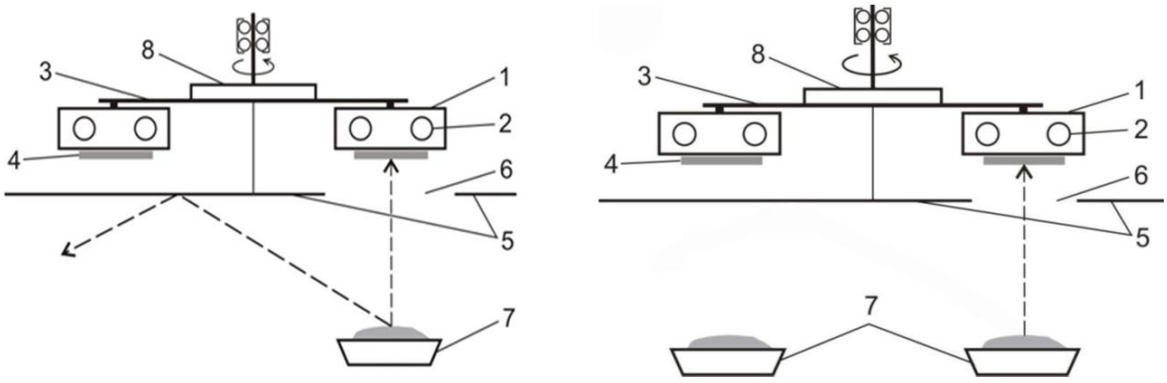

Fig. 1. Scheme of the device for films (a) and two-layer structures deposition (b): 1 – the system of micro heaters, 2 – heaters, 3 – radial brackets, 4 – substrate for steam deposition, 5 – shutter, 6 – asymmetric hole, 7 – evaporator, 8 – the mechanical system for microheaters rotating.

of two-layer thin-film structures. For this purpose, the second evaporator begins to heat when the shutter is blocked, then a hole in the shutter places to the front of the second evaporator and one of the microheaters with deposited condensate find a place according to the procedure described above. After depositing time of the second layer of another material shutter blocks steam from the second evaporator and the next microheater is replaced. After that, the shutter opens and the process repeats. After mentioned above process, the shutter is blocked and the second evaporator is switched off.

2.2. Morphology properties of CdTe thin films

It should be noted, that condensed structures in vacuum characterized by a certain specificity associated with significant supercooling and vapor saturation in comparison with the crystallization conditions of massive crystals and numerous physical and technological parameters, that affect the kinetics of their formation. The latter include the following:

• Temperature of evaporation, which determines the state of the vapor particles and their energy, which can affect the formation processes of both the initial and subsequent condensation stages;

• Substrate temperature is one of the most important parameters that determine the mechanisms of condensation and growth, the degree of phase structural and substructural imbalanced, especially during condensation vapor on amorphous substrates;

• The ratio between the substrate temperature and temperature of evaporator determine the quality of the film obtained [21];

• Physicochemical characteristics of the substrate determine the structural (amorphous, polycrystalline, or single crystalline) and substructural state, the surface quality of the condensate, topology.

Thin films on a glass substrate obtained by the PVD technique. The temperature of evaporation was T_E = (790-850) K and condensation T_S = 470 K. Thickness of films was controlled by time of vapor deposition from 160 to 570 s. Technological parameters are shown in Table 1. In addition to surface morphology and profilograms (Figures 2 - 3) AFM studies determined the size of nanocrystals, roughness, and other characteristics of the obtained condensates (Table 3).

If in the initial stages of deposition of the CdTe thin film N20 (Fig. 3, a), separate columnar nanoparticles are formed as a “fish scale” with a maximum height of ~ 70 nm before and ~ 15 nm after annealing (Fig. 3b). The average height values also decrease after annealing from ~ 33 nm to ~ 9 nm. This step-by-step formation of nanostructures is related to their layered growth, which is accompanied by processes of nucleation, aggregation, and subsequent growth of nanocrystallites [13]. After annealing, the coalescence mode is observed (Fig. 2b; Fig. 3b) can be observed mergers and, as a result, a decrease in the density of nanostructures: nanostructures finally merged and created a solid condensate.

Now, in relation to other characteristics obtained of the nanostructures: the average surface roughness of the condensate varies with size. For as-grown films, the value is ~ 1.291 nm and after annealing ~ 0.541 nm (Fig. 3, a-b).

Table 3

Structural properties of CdTe N20 thin films.

Sample, CdTe N20/glass	as grown	after annealing
h max, nm	70.38	15.48
<h>, nm	33.30	9.10
R_a	1.291	0.541
R_{ms}	2.397	0.732

In this case, the CdTe thin films on a glass substrate grown of the nanostructure are realized by the Folmer-Weber mechanism, which is confirmed by the results of AFM images (Fig. 2, Fig. 3). Herewith, in most cases, columnar structures are formed, the sizes and structural shapes are determined by the temperature of evaporation and time of deposition.

2.3. Optoelectronic studies

Recrystallization of Cadmium Telluride thin films is highly depending on the annealing effect, altering many properties like intrinsic defects and stress, crystallite size, slightly shifting the optical absorption edge [41]. The most important tools of determining the band structure of semiconductors is understanding the

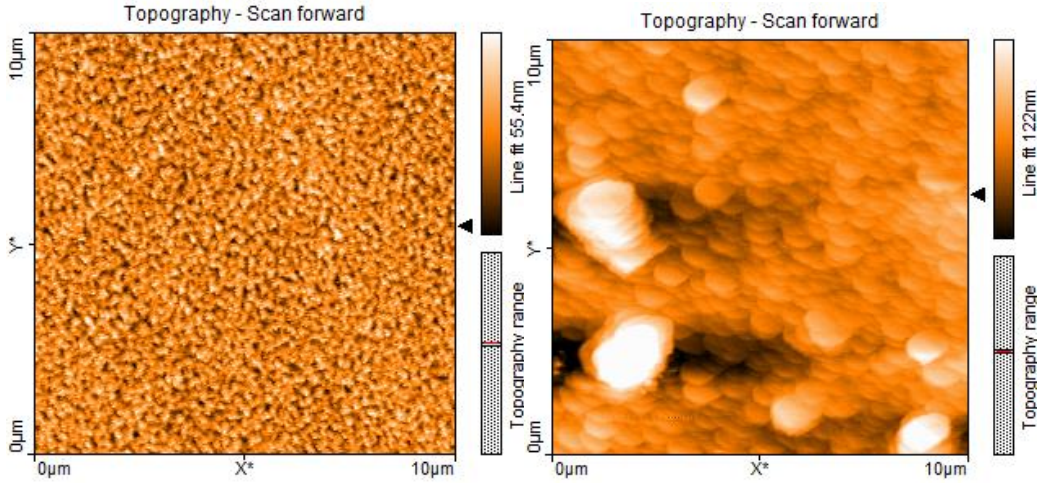

a) *b)*

Fig. 2. AFM images of CdTe N20 thin films on glass size 10x10 µm for as grown (a) and after annealing (b).

a)¶

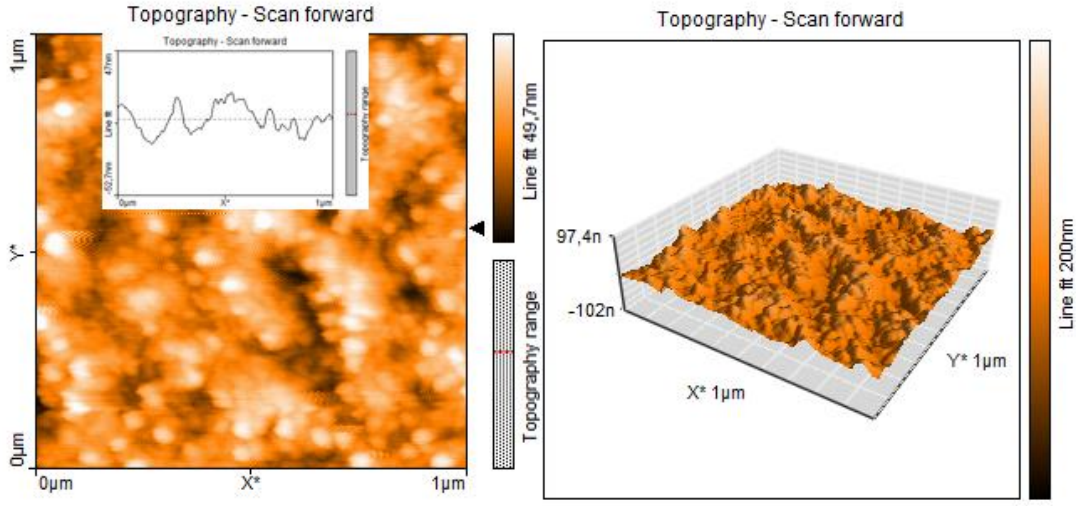

b)¶

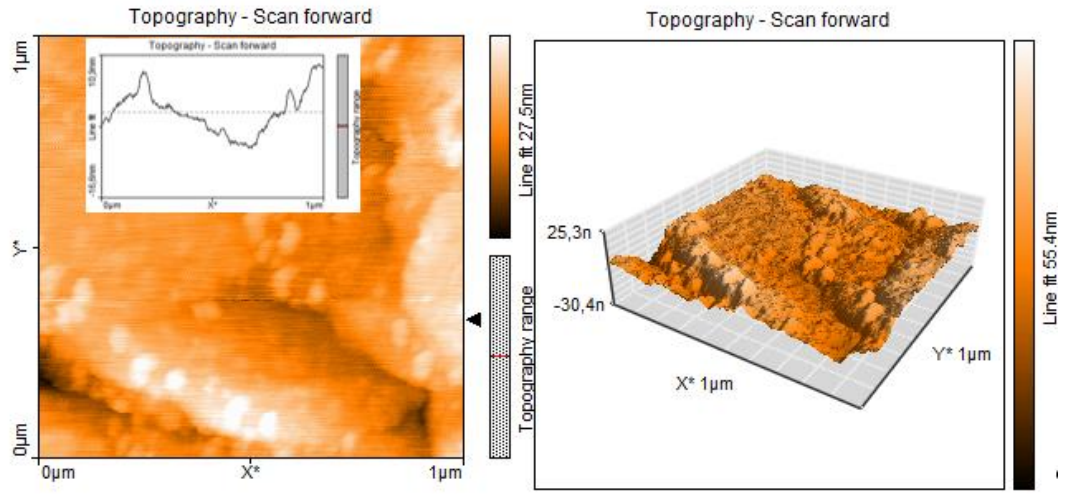

Fig.3. AFM images of CdTe N20 on glass size 1x1 µm for as grown (a) and after annealing (b).

behavior of optical properties with annealing temperature [41-42].

Optical studies of the films have been carried out using the transmittance spectra of the films in the spectral range 180-3300 nm (Fig.4, a). It can be seen from Fig. 4, a), then the transmittance spectrum of the films shows interference fringes with a sharp fall at the band edge in the wavelength region 805 - 3300 nm; whereas the interference effects disappear below this region. The area of the transparency of samples begins near 790-805 nm

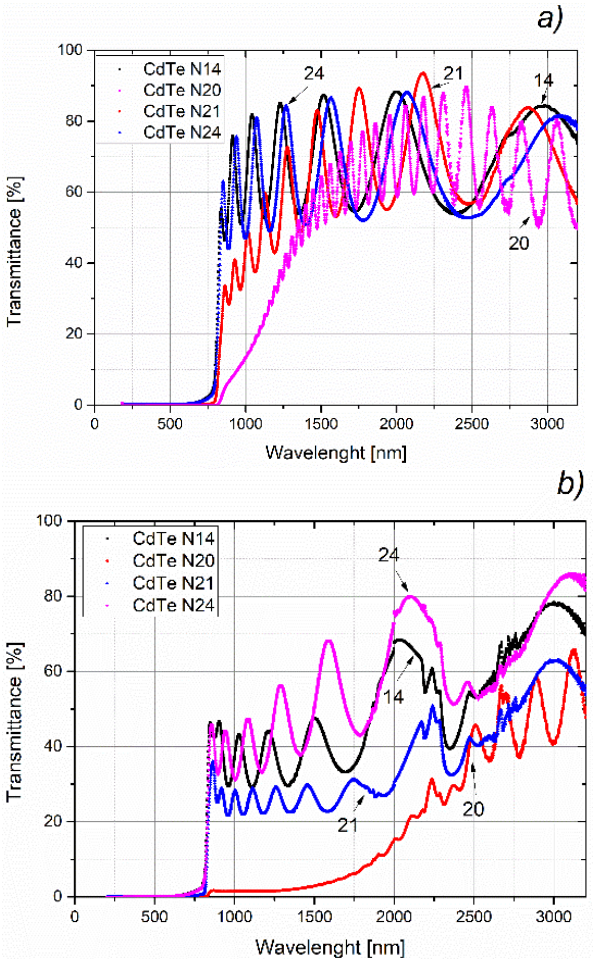

Fig. 4. Transmission spectra of as grown (a) and after annealing (b) CdTe thin films.

depending on the sample. It is clearly observed that the absorption edge is shifted to the long wavelength area as the thickness of samples increases (Fig. 4, a). It is known that in the absorption process, a photon of known energy excites an electron from lower to higher energy state, corresponding to absorption edge [43].

All films above the absorption edge have high transparent in range 85 - 90 %. Using uniformly consistent maximum and minimum of the interference pattern in the transparent region, can be speak about the optical homogeneity of the deposited films [42].

The difference between the position of absorption edge of the N14, N21, N24 films was destroyed after the annealing at 723 K (Fig. 4, b), but the absorption edge of N20 sample lies much further in the long wavelength area than for another samples. Beginning of transparency area in the transmission spectrum of these samples is shifted and a remarkable decrease in the transmission of annealed films is observed. In general, decrease in the transmittance of thin films is mainly related with the change of surface morphology, with the grain structure and with the defect density [44, 45]. After annealing a decrease of the average transmission values (increase of absorption) can be due mainly by increasing in grain size [45-46]. We note that N. Kim [36] was shown, that laser annealing of CdTe layer resulted in an increase of grain size and a decrease of surface roughness.

The optical band gap energies of CdTe thin films for different thickness were calculated using the Tauc formula [47]

$$(\alpha h\nu)^2 = A(h\nu - E_g) \qquad (2)$$

$h\nu$ – photon energy; E_g is the optical energy band gap, A is an energy-independent constant.

The optical band gap energies of the as grown and the annealing CdTe thin films were evaluated by extrapolating the linear region of each curve back to the energy axis from the Tauc plot of $(\alpha h\upsilon)^2$ vs. the photon energy $(h\upsilon)$ [48, 49], as shown in the Fig. 5, a and Fig 5, b. The optical band gap energies of as grown CdTe thin films of different thickness were 1.50; 1.41; 1.46 and 1.49 eV for the samples N14, N20, N21 and N24, respectively. After annealing the optical band gap is 1.46 eV for all samples. The decrease of the optical energy gap for samples N14 and N24 can be, in general, correlated with the increase of the absorbance as a result of increasing the film crystallinity due to the increase of the grain size values [45, 36, 48].

For analysis of optical spectra, the absorption coefficient has been calculated using the Envelope Method (EM) developed by Swanepoel [49 – 50]. By the interference patterns can be calculated d, n, α, s, λ and T denote the thickness of films, refractive index, absorption coefficient, substrate refractive index, wavelength and transmission of the film, respectively.

Refractive index is one of the fundamental properties of materials as it is closely related to the electronic polarizability of ions, local field inside the material as well as the transmittance [51]. In this method, the extrema of interference fringes in transmittance spectra is using to calculate n using the relation, which is based on Swanepoel method [50]:

$$n = \left[N + (N^2 - s^2)^{1/2}\right]^{1/2} \qquad (3)$$

$$N = \frac{2s(T_M - T_m)}{T_M T_m} + \frac{(s^2+1)}{2} \qquad (4)$$

where N is the Swanepoel coefficient and s is the refractive index of the substrate. The dispersion of refractive index with respect to wavelength for as grown CdTe thin films and after annealing films is shown in Figure 4. Complex refractive index can be written as $n_c = n + ik$ where, n and k are refractive index and extinction coefficient, respectively [41]. The increase of the refractive index associated with the packing density increase and the improvement of the crystallinity of layers as results their thickness are increase earlier observed for CdTe obtained by electron beam evaporation technique [45]. For the sample N14 (Fig. 6, a) the calculated refractive index before annealing is practically constant, but after annealing the value of "n" strongly depend on wavelength above 1800 nm.

The opposite situation applies to the sample N21 (Fig. 6, b). Before annealing the refractive index shown normal dispersion, whereas after annealing is practically independent wavelength. For sample N20 (Fig. 6, b) before annealing the strong a normal dispersion is observed, but after annealing the value of refractive index practically not depend on wavelength in the region above 2500 nm. We note that the calculation of refractive

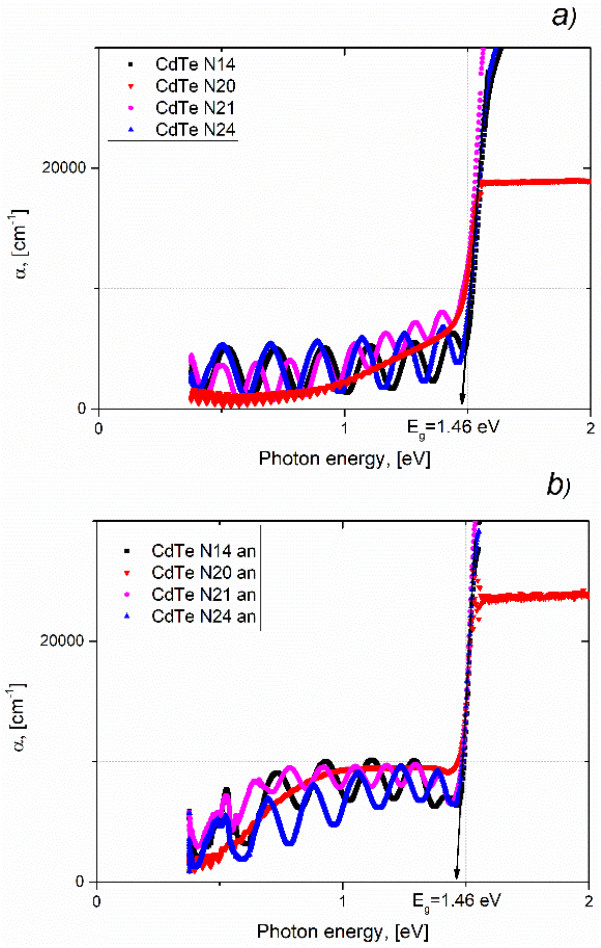

Fig. 5. Absorption spectra in Tauc coordination's of as grown (a) and after annealing (b) CdTe thin films.

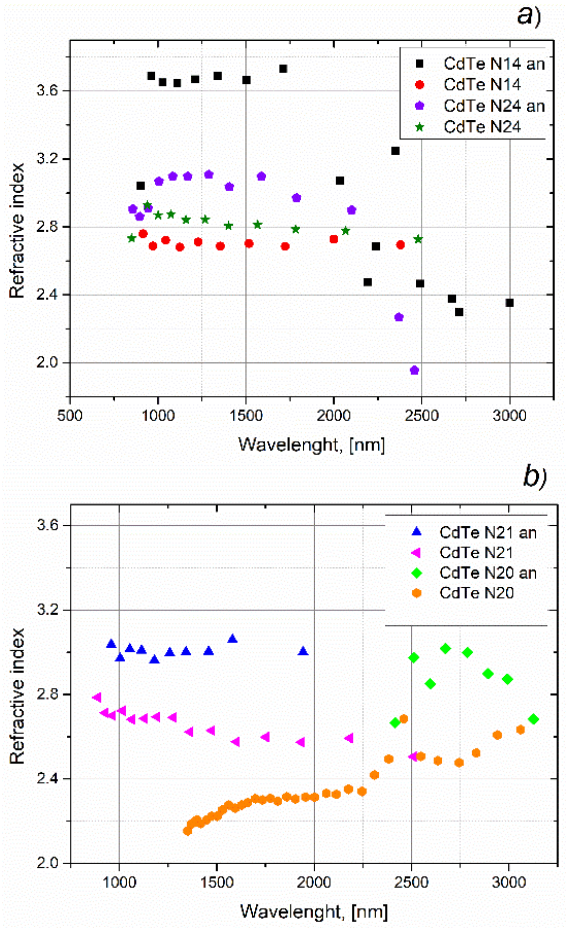

Fig. 6. Refractive index (n) of dispersion spectra for as grown and annealing (an) CdTe thin films: a) samples N14 and N24; b) samples N21 and N20.

index below 2500 nm is not possible because interference pattern is not observed.

n_1 and n_2 are the refractive indexes at extremum of interference fringes two adjacent maxima (or minima) at wavelength λ_1 and λ_2, respectively [52]. In this case the thickness can be calculated as:

$$d = \frac{\lambda_1 \lambda_2}{2(\lambda_1 n(\lambda_2) - \lambda_2 n(\lambda_1))} \quad (5)$$

The average values of theoretical thickness calculated by Swanepoel's method is 1218,52 nm for the sample N14/ after annealing 1333,39 nm (experimental value is 1215 nm) and 1640,92 nm/ after annealing 1540,68 nm for the sample N 21 (experimental is 1565 nm). The measured values of the thickness were received using the profilometer method (Table 1). By comparing the experimental and calculated values of the thickness, it can be noted that a small difference in value is associated with the error of the thickness calculation and experimental measurement.

In order to calculate the other relevant optical constant, namely, absorbance (x) it was estimated using Eq. (6) which derived from the Connell and Lewis method [50, 51]:

$$x = \frac{P + [P^2 + 2QT_a(1 - R_2R_3)]^{1/2}}{Q} \quad (6)$$

where,

$$Q = 2T_a(R_1R_2 + R_1R_3 - 2R_1R_2R_3 \quad (7)$$

$$P = (R_1 - 1)(R_2 - 1)(R_3 - 1) \quad (8)$$

$$R_1 = \left[\frac{1-n}{1+n}\right]^2 \quad (9)$$

$$R_2 = \left[\frac{n-s}{n+s}\right]^2 \quad (10)$$

$$R_3 = \left[\frac{s-1}{s+1}\right]^2 \quad (11)$$

Using the calculated x, the absorption coefficient (α) was determined by the formula [48]:

$$x = \exp(-\alpha d) \quad (12)$$

The absorption coefficient α is a criterion to demonstrate the capability of semiconductor to absorb photons. The obtained values of α from Swanepoel's method illustrated in Figure 7. After annealing increase of absorption coefficient can be observed for samples N14 and N21 (Fig. 7, a) and increase of the optical conductivity for the samples N24_an (Fig. 7, b). General absorption values for the samples remained low compared to as grown and is attributed to optical absorption of free Te released on the film surfaces. That absorbance increased for samples N14_an and N21_an is

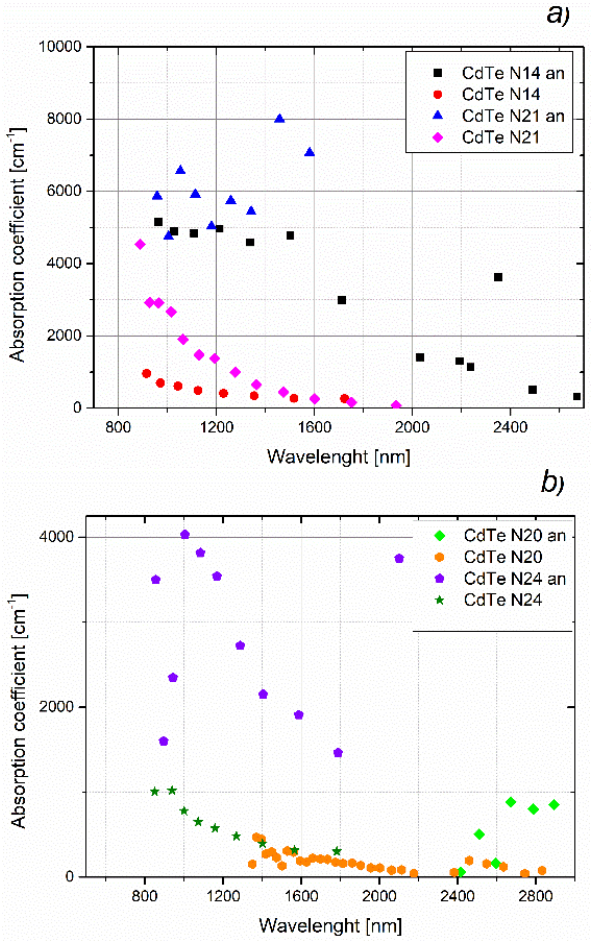

Fig. 7. Absorption coefficient (α) of dispersion spectra for as grown and annealing (an) CdTe thin films.

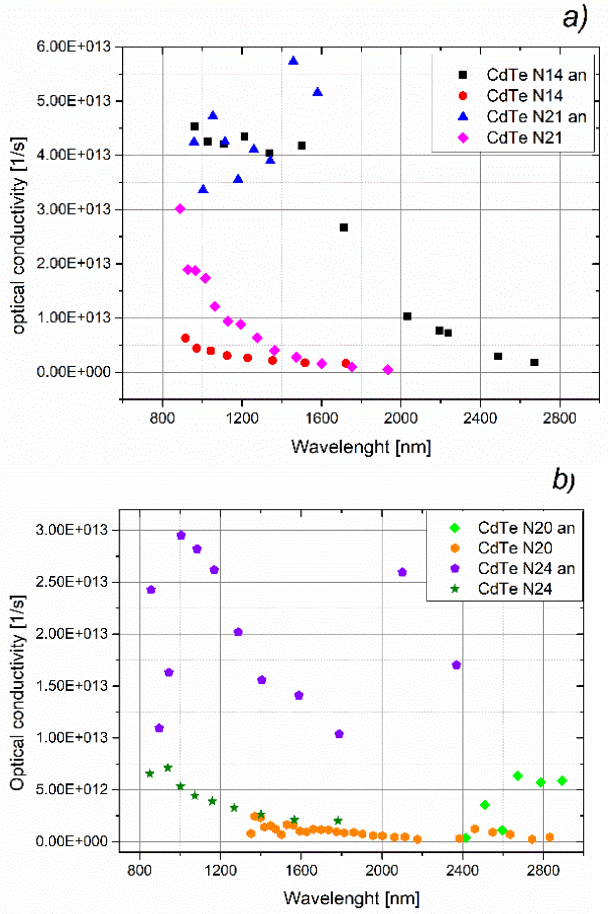

Fig. 8. The optical conductivity against photon wavelength for the as grown and annealing CdTe thin films

because of conversion of Te into TeO_2 after the oxidation process [52].

The extinction coefficient, k provides information about the absorption of light in the bulk of the material due to inelastic scattering [49]. Extinction coefficient was calculated using the formula [53]:

$$k = \frac{\alpha\lambda}{4\pi} \tag{13}$$

According to the Figure 8, *k* decreases after increasing of wavelength (for the samples N14 and N21). Furthermore, the calculated values *k* illustrates highest extinction coefficient for films annealed at 723 K for samples N21_an and 24_an (Fig. 8).

The range of refractive indices from 2.70 to 3.10 reported in works Myers et al. [54], Khairnar et al. [55] and Kosyachenko et al. [56] and the variation of extinction coefficient from about 0 to 0.5 CdTe films deposited at different temperature. Therefore, it reveals that present results consistent for the refractive index while for Extinction coefficient the range of variation is much narrower. This may be attributed to the particular structure of films and their thicknesses.

Optical conductivity is one of the main parameters for studying electronic states in thin-film materials [47, 53]. If to the system an external electric field is applied, as a rule, the charge begins to redistribute and currents are induced. For small enough fields, the induced polarization and the induced currents are proportional to the inducing field. The optical conductivity of the different thickness of CdTe is calculated by equation:

$$\sigma_{opt} = \frac{\alpha n c}{4\pi} \tag{14}$$

where α is the absorption coefficient, n is the refractive index and *c* is the velocity of light.

Figure 8 shows the variation of the optical conductivity upon the wavelength for CdTe thin films. It is observed that the optical conductivity increases after annealing which could be related to the increase in the refractive index and the density of localized states in the gap due to the appearance of new defects states [28].

Conclusions

The paper considers the obtaining of thin films using PVD technique. It is discussed how the main technological parameters affect the optical properties and the quality of film obtaining. Thin films of Cadmium Telluride on glass substrates were obtained using an optimized thermal evaporation method. The films are grown on glass substrates with different technological parameters (temperature of evaporation and time of deposition). Later, for the correction of the surface structure of the film, they were annealed at a temperature of 723 K. Optoelectronic properties, such as absorption coefficient, optical conductivity, refractive index and thickness, were investigated from the transmission spectra for as-grown and annealing films by the Swanepoel method. It was observed that the surface of

thin films is homogeneity as evidenced by interference patterns. It is established that after annealing films are characterized by slightly lower values of transmission, but they are characterized by better values of absorption coefficient. This is primarily due to the fact that after the annealing grains on the surface of the film sintered in larger ones, and also at high annealing temperature the free phases of Te are observed on the surface of the film. The annealing films are characterized by high values of the coefficient of absorption and it is about 10^4 cm^{-1}.

Yavorskyi R.S. – PhD Student, Department of Physics and Chemistry of Solids.

[1] F.L. Luo and Ye Hong, Renewable energy systems: advanced conversion technologies and applications, Crc Press, (2016).
[2] J. Appelbaum, Renewable and Sustainable Energy Reviews 81, 161 (2018) (doi:10.1016/J.RSER.2017.07.026).
[3] G. Wisz, L. Nykyruy, V. Yakubiv, I. Hryhoruk, R. Yavorskyi, International Journal of Renewable Energy Research (IJRER) 8(4), 2367 (2018).
[4] G. Wisz, I. Virt, P. Sagan, I. Hatala, Ł. Głowa, M. Kaczor, R. Yavorskyi, Standard Si Photovoltaic Devices Improved by ZnO Film Obtained by Pulsed Laser Deposition. Fesenko O., Yatsenko L. (eds) Nanophysics, Nanomaterials, Interface Studies, and Applications. NANO 2016, Springer Proceedings in Physics, vol 195. Springer, Cham, (2017) (doi:10.1007/978-3-319-56422-7_24).
[5] P. Sampaio, M. González, Renewable and Sustainable Energy Reviews. 74, 590 (2017) (doi:10.1016/J.RSER.2017.02.081).
[6] M.A. Green, Y. Hishikawa, W. Warta, et al., Prog Photovolt Res Appl. 25(7), 668 (2017). (doi:10.1002/pip.2909).
[7] A. Polman, M. Knight, E.C. Garnett, B. Ehrler, W.C. Sinke, Science 352(6283), aad4424 (2016) (doi:10.1126/science.aad4424).
[8] U. Gangopadhyay, S. Jana, S. Das, State of Art of Solar Photovoltaic Technology, In: Proceedings of International Conference on Solar Energy Photovoltaics 2013, 1 (2013) (doi:10.1155/2013/764132).
[9] H. Il'chuk, A. Kashuba, R. Petrus, I. Semkiv, & N. Ukrainets. Simulation the spectral dependence of the transmittance for semiconductor thin films. Physics and Chemistry of Solid State, 21(1), 57 (2020). (doi:10.15330/pcss.21.1.57-60).
[10] J. D. Major, et al., Nature 511(7509), 334 (2014) (doi:10.1038/nature13435).
[11] T. Suntola, MRS Bulletin 18(10), 45 (1993) (doi:10.1557/S088376940003829X).
[12] L. Nykyruy, Ya. Saliy, R. Yavorskyi, Ya. Yavorskyi, G. Wisz, Sz. Górny, V. Schenderovsky, 2017 IEEE 7th International Conference Nanomaterials: Application & Properties (NAP), At Odesa, Ukraine. 01PCSI26-1-01PCSI26-5 (2017) (doi:10.1109/NAP.2017.8190161).
[13] Y.P. Saliy, L.I. Nykyruy, R.S. Yavorskyi, S. Adamiak, Journal of Nano- and Electronic Physics 9 (5), 05016 (2017) (doi:10.21272/jnep.9(5).05016.
[14] R.Y. Petrus, H.A. Ilchuk, A.I. Kashuba, et al. Optical-Energy Properties of CdS Thin Films Obtained by the Method of High-Frequency Magnetron Sputtering. Opt. Spectrosc. 126, 220 (2019). (doi:10.1134/S0030400X19030160).
[15] A.A. Ojo, I.M. Dharmadasa, Solar Energy 136, 10 (2016) (doi:10.1016/j.solener.2016.06.067).
[16] W. Cyrs, H. Avens, Z. Capshaw, R. Kingsbury, J. Sahmel et. al., Energy Policy 68, 524 (2014) (doi:10.1016/J.ENPOL.2014.01.025).
[17] K. Chopra, S. Das, Thin Film Solar Cells. Springer, Boston, MA, pp. 275 (1983) (doi:10.1007/978-1-4899-0418-8_6).
[18] T.M. Mazur, V.P. Makhniy, V.V. Prokopiv, M.M. Slyotov, Journal of Nano- and Electronic Physics, 9(5), 05047 (2017) (doi: 10.21272/jnep.9(5).05047).
[19] T.M. Mazur, V.V. Prokopiv, M.M. Slyotov, M.P. Mazur, O.V. Kinzerska, O.M. Slyotov, Physics and Chemistry of Solid State 21(1), 52 (2020) (doi: 10.15330/pcss.21.1.52-56).
[20] V. Krishnakumar, B. Späth, C. Drost, C. Kraft, B. Siepchen, A. Delahoy, O. Zywitzki, Thin Solid Films 633, 112 (2017) (doi:10.1016/j.tsf.2016.10.009).
[21] R.S. Yavorskyi, Z.R. Zapukhlyak, Ya.S. Yavorskyi, L.I. Nykyruy, Physics and chemistry of solid state 18(4), 410 (2017) (doi:10.15330/pcss.18.4.410-416).
[22] S. Singh, R. Kumar, K.N. Sood, Thin Solid Films 519(3), 1078 (2010) (doi:10.1016/J.TSF.2010.08.047).
[23] V.V. Brus, M.N. Solovan, E.V. Maistruk, I.P. Kozyarskii, P.D. Maryanchuk, K.S. Ulyanytsky, J. Rappich, Physics of the Solid State 56(10), 1947 (2014) (doi:10.1134/S1063783414100072).
[24] S. Lalitha, S.Z. Karazhanov, P. Ravindran, S. Senthilarasu, R. Sathyamoorthy, J. Janabergenov, Physica B: Condensed Matter 387(1-2), 227 (2007) (doi:10.1016/J.PHYSB.2006.04.008).
[25] X. Wu, Solar energy 77(6), 803 (2004) (doi:10.1016/J.SOLENER.2004.06.006).
[26] F. Hosseinpanahi, D. Raoufi, K. Ranjbarghanei, B. Karimi, R. Babaei, E. Hasani, Applied Surface Science 357, 1843 (2015) (doi:10.1016/J.APSUSC.2015.09.048).

[27] R. Kulkarni, S. Rondiya, A. Pawbake, R. Waykar, A. Jadhavar, V. Jadkar, S. Jadkar, at al., Energy Procedia 110, 188 (2017) (doi:10.1016/J.EGYPRO.2017.03.126).
[28] X. Wen, C. Chen, S. Lu, K. Li, R. Kondrotas, Y. Zhao, et al., Nature communications 9(1), 2179 (2018) (doi:10.1038/s41467-018-04634-6).
[29] O. Vigil-Galán, M. Courel, F. Cruz-Gandarilla, D. Seuret-Jiménez, Journal of Materials Science: Materials in Electronics 27(6), 6088 (2016) (doi:10.1007/s10854-016-4534-1).
[30] Rugen-Hankey, S. L., et al. Solar Energy Materials and Solar Cells 136, 213 (2015).
[31] G. Kartopu, L. Phillips, V. Barrioz, S. Irvine, S. Hodgson, et. al., Progress in Photovoltaics: Research and Applications 24(3), 283 (2016) (doi:10.1002/pip.2668).
[32] J. Major, Y. Proskuryakov, K. Durose, G. Zoppi, I. Forbes, Solar Energy Materials and Solar Cells 94(6), 1107 (2010) (doi:10.1016/J.SOLMAT.2010.02.034).
[33] T. Baines, T. Shalvey, J. Major, A Comprehensive Guide to Solar Energy Systems 215 (2018) (doi:10.1016/B978-0-12-811479-7.00010-)5.
[34] M. Ruiz-Preciado, M.A. Quevedo-Lopez, A.G. Rojashernandez, et al., Digest journal of nanomaterials & biostructures (DJNB) 12(4), 1057 (2017).
[35] X. Yang, B. Liu, B. Li, J. Zhang, W. Li, L. Wu, L. Feng, Applied Surface Science 367, 480 (2016) (doi:10.1016/J.APSUSC.2016.01.224).
[36] N. Kim, C. Park, J. Park, Journal of the Korean Physical Society 62(3), 502 (2013) (doi:10.3938/jkps.62.502).
[37] S. Tadashi, M. Sunao, M. Shigekazu, Japanese Journal of Applied Physics 16(5), 807 (1977).
[38] A. Salavei, I. Rimmaudo, F. Piccinelli, A. Romeo, Thin Solid Films535, 257 (2013) (doi:10.1016/j.tsf.2012.11.121).
[39] J.A. Venables, G.D.T. Spiller, M. Hanbucken, Reports on progress in physics 47(4), 399 (1984).
[40] D.M. Freik, Ya.S. Yavorskyi, V.Y. Potyak, R.S. Yavorskyi, Physics and Chemistry of Solid State 13(2), 509 (2012).
[41] R. Yu. Petrus, H. A. Ilchuk, A. I. Kashuba, optical properties of CdS thin films, Journal of Applied Spectroscopy. 87(1), 35 (2020) (doi:10.1007/s10812-020-00959-7).
[42] E. Akbarnejad, M. Ghoranneviss, S. Mohajerzadeh, M.R. Hantehzadeh, E. Asl. Soleimani Journal of Physics D: Applied Physics 49(7), 5301 (2016).
[43] K.S. Bindra, Nikhil Suri, R. Thangaraj, Chalcogenide Let. 3(9), 133 (2006).
[44] L.I. Nykyruy, R.S. Yavorskyi, Z.R. Zapukhlyak, G. Wisz, P. Potera. Optical Materials 92, 319 (2019) (doi:10.1016/j.optmat.2019.04.029).
[45] H.H. Güllü, I. Candan, E. Coşkun, M. Parlak, Optik-International Journal for Light and Electron Optics 126(18), 1578 (2015) (doi:10.1016/J.IJLEO.2015.05.026).
[46] M.M. Abd El-Raheem, H.M. Ali, N.M. El-Husainy, Journal of Optoelectronics and Advanced Materials 11(6), 813 (2009).
[47] J. Tauc (ed.), Amorphous and liquid semiconductors (Springer Science & Business Media, 2012).
[48] C.V. Ramana, R.J. Smith, O.M. Hussain, Physica status solidi (a) 199(1), 4 (2003) (doi:10.1002/pssa.200309009).
[49] R. Yavorskyi, L. Nykyruy, G. Wisz, P. Potera, S. Adamiak, Sz. Górny, Applied Nanoscience 1, 10 (2018) (doi:10.1007/s13204-018-0872-z).
[50] R. Swanepoel, Journal of Physics E: Scientific Instruments 17(10) 896 (1984) (doi:10.1088/0022-3735/17/10/023).
[51] R.R. Reddy, Y. Nazeer Ahammed, K. Rama Gopal, D.V. Raghuram, Optical Materials. 10(2), 95 (1998) (doi:10.1016/S0925-3467(97)00171-7).
[52] J.D. Major. Semiconductor Science and Technology 31(9), 093001 (2016) (doi:10.1088/0268-1242/31/9/093001).
[53] G.A.N. Connell, A. Lewis, Physica status solidi (b) 60(1), 291 (1973) (doi:10.1002/pssb.2220600132).
[54] T.H. Myers, S.W. Edwards, J.F. Schetzina, Journal of Applied Physics 52, 4231 (1981) (doi:10.1063/1.329272).
[55] U.P. Khairnar, D.S. Bhavsar, R.U. Vaidya, G.P. Bhavsar, Materials Chemistry and Physics 80(2), 421 (2003) (doi:10.1016/s0254-0584(02)00336-x).
[56] L.A. Kosyachenko, E.V. Grushko, X. Mathew, Solar Energy Materials and Solar Cells 96, 231 (2012) (doi:10.1016/j.solmat.2011.09.063).

Р.С. Яворський

Особливості оптичних властивостей високостабільного шару CdTe як фотоелектричного абсорбційного шару

Прикарпатський національний університет імені Василя Стефаника,
Івано-Франківськ, Україна. roctyslaw@gmail.com

У роботі досліджено технологію отримання та вплив ефект відпалу на морфологію та оптичні властивості тонких плівок телуриду кадмію. Вивчено вплив режимів осадження на ріст тонких плівок. Для отриманих тонких плівок телуриду кадмію використовували модифікований метод термічного випаровування, нанесений технікою фізичного осадження пари на скляну підкладку різної товщини. Вимірювання пропускання проводили за допомогою спектрофотометра UV-ViS-NIR в діапазоні довжин хвиль 180-3300 нм для аналізу оптичних властивостей як функції довжини хвилі. Значення ширини забороненої зони – 1,49 еВ для вирощених плівок та 1,46 еВ після відпалу. Показники заломлення зразків були визначені в діапазоні 2,6 - 2,8 для вирощених плівок, і їх значення дещо зросли після відпалу в залежно від області довжини хвилі та товщини плівки. Після відпалу спостерігається коалесценційний режим росту.

Ключові слова: метод термічного випаровування, метод Сванеполя, тонкі плівки телуриду кадмію, оптичні властивості, сонячні елементи, ефект відпалу.